

Article

Fabrication of Hydroxypropyl Methylcellulose Orodispersible Film Loaded Mirtazapine Using a Syringe Extrusion 3D Printer

Tanpong Chaiwarit¹, Niphattha Aodsab¹, Pimonnart Promyos¹, Pattaraporn Panraksa¹ , Suruk Udomsom² 
and Pensak Jantrawut^{1,3,*} 

¹ Department of Pharmaceutical Sciences, Faculty of Pharmacy, Chiang Mai University, Chiang Mai 50200, Thailand

² Biomedical Engineering Institute, Chiang Mai University, Chiang Mai 50200, Thailand

³ Cluster of Research and Development of Pharmaceutical and Natural Products Innovation for Human or Animal, Chiang Mai University, Chiang Mai 50200, Thailand

* Correspondence: pensak.amuamu@gmail.com or pensak.j@cmu.ac.th

Abstract: Depression is a mental illness causing a continuous negative feeling and loss of interest and affects physical and mental health. Mirtazapine (MTZ) is an effective medicine for treating depression, but patients lack compliance. However, transforming a pharmaceutical dosage form to an orodispersible film (ODF) could resolve this issue. This study aims to fabricate ODF-loading mirtazapine, using a syringe extrusion 3D printer, and compare its properties with the solvent-casting method. The ODFs were prepared by dissolving the mirtazapine in a hydroxypropyl methylcellulose E15 solution, and then fabricated by a 3D printer or casting. The 3D printing was accurate and precise in fabricating the ODFs. The SEM micrographs showed that the mirtazapine-printed ODF (3D-MTZ) was porous, with crystals of mirtazapine on the film's surface. The 3D-MTZ exhibited better mechanical properties than the mirtazapine-casted ODF (C-MTZ), due to the 3D-printing process. The disintegration time of the 3D-MTZ in a simulated salivary fluid, pH 6.8 at 37 °C, was 24.38 s, which is faster than the C-MTZ (46.75 s). The in vitro dissolution study, in 0.1 N HCl at 37 °C, found the 3D-MTZ quickly released the drug by more than 80% in 5 min. This study manifested that 3D-printing technology can potentially be applied for the fabrication of ODF-containing mirtazapine.

Keywords: orodispersible film; 3D-printing; hydroxypropyl methylcellulose; mirtazapine; depression



Citation: Chaiwarit, T.; Aodsab, N.; Promyos, P.; Panraksa, P.; Udomsom, S.; Jantrawut, P. Fabrication of Hydroxypropyl Methylcellulose Orodispersible Film Loaded Mirtazapine Using a Syringe Extrusion 3D Printer. *Sci. Pharm.* **2022**, *90*, 68. <https://doi.org/10.3390/scipharm90040068>

Academic Editor: Roman B. Lesyk

Received: 6 October 2022

Accepted: 21 October 2022

Published: 26 October 2022

Publisher's Note: MDPI stays neutral with regard to jurisdictional claims in published maps and institutional affiliations.



Copyright: © 2022 by the authors. Licensee MDPI, Basel, Switzerland. This article is an open access article distributed under the terms and conditions of the Creative Commons Attribution (CC BY) license (<https://creativecommons.org/licenses/by/4.0/>).

1. Introduction

Major depressive disorder or depression is a compound mood disorder and a serious mental health problem. According to the World Health Organization (WHO), people around the world (about 280 million) have depression. During a depressive episode, the patients are in a depressed mood, including feeling of sadness, irritableness and emptiness, and a loss of interest in activities. Other symptoms are a loss of concentration, feelings of excessive guilt, feeling low in energy, changing sleep behaviour, changes in weight or appetite, low self-esteem, and hopelessness. Depression can also affect patients to suffer greatly and function poorly in society. Importantly, it can lead to suicide [1].

Mirtazapine (MTZ), [\pm]-2-methyl-1,2,3,4,10,14b-hexahydropyrazino [2,1-a] pyrido [2,3-e] benzazepine, is considered to be a safe and versatile antidepressant [2,3], which is used in hospitals to cure moderate to severe depression and anxiety. MTZ is insoluble in water, with a logarithm partition coefficient (octanol–water) of 2.9. This indicates a high hydrophobicity, but it does dissolve in ethanol and an acidic condition. The MTZ has a low bioavailability (50%), high protein-binding (85%), and a long half-life (20–40 h) [4]. MTZ has a relatively narrow therapeutic index and should be individually optimized to obtain a therapeutic effect [5]. Its chemical structure is presented in Figure 1. Generally, tablets are the available dosage form of MTZ in doses of 15, 30, and 45 mg, respectively. The tablet dosage form lacks patient compliance in long-term use. It is also unsuitable for

patients who cannot swallow a tablet and are uncooperative with treatment in physiological therapy centres. Furthermore, in the hospital, the pharmacy compounding of the MTZ liquid formulation was done by crushing tablets in a mortar to a fine powder and mixing with the vehicle until the liquid was formed. The suspension of MTZ was then transferred into a container. The main disadvantage of the compounded MTZ liquid formulation is its homogeneity, which may affect the dose accuracy.

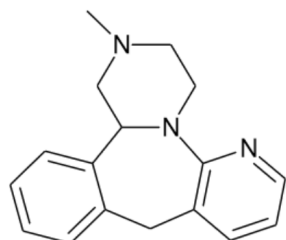


Figure 1. Chemical structure of mirtazapine.

Orodispersible films (ODFs) have been developed to overcome the compliance problem. ODF is a thin film, loaded with a drug, for the fast disintegration of a dosage form in the oral cavity immediately after placing on the tongue [6]. It is simple to administer oral drugs for paediatric and geriatric patients with swallowing difficulties [7]. ODFs are generally produced by the solvent-casting method, preparing a film by dissolving a drug and polymer in a solvent, and casting it onto a plate and drying [8].

Three-dimensional (3D) printing technology is a novel and exciting technology in the pharmaceutical field, since it is able to produce several pharmaceutical formulations, which are designed in the desired shape and size, and customize a drug for a specific patient [9,10]. The extrusion (solid or semi-solid)-based printing technique is one of the most well-known 3D-printing techniques to produce novel, solid pharmaceutical dosages, such as polypills, multilayer tablets, floating drug delivery platforms, and orodispersible films (ODFs), because of its high capacity to load a drug, its low-cost and capability to print a 3D object with various types of polymers at room temperature [11,12]. Furthermore, the 3D printing can fabricate a dosage form with a highly accurate drug content because it can calculate the material consumption to control or adjust the dose of the drug. This property is appropriate for a relatively narrow therapeutic index and personalized medicines, such as MTZ. Thus, 3D printing can resolve the drug accuracy issue of MTZ.

Various polymers, such as polyvinylpyrrolidone (PVP), polylactic acid (PLA), polyvinyl alcohol (PVA) and hydroxypropyl methylcellulose (HPMC), can be applied for ODFs preparation with the 3D-printing technique [13,14]. HPMC is a hydrophilic polymer that dissolves in water and ethanol. It is widely used as an excipient in pharmaceutical applications for several functions, such as a binder, suspending agent, thickening agent, gelling agent, and film-forming agent. HPMC is classified by several factors, such as viscosity and degree of substitution. HPMC E15, that is, low-viscosity HPMC, is used for ODFs preparation and is appropriate for extrusion based-3D printing to produce an oral dosage form [13,15,16]. In a previous study, HPMC E15 and pregelatinized starch ODFs containing levocetirizine dihydrochloride showed an ability to be used for semi-solid extrusion 3D printing. It manifested good mechanical properties and rapidly released the levocetirizine dihydrochloride from the formulation [17].

Consequently, the present study investigated mirtazapine ODFs fabricated by a syringe extrusion 3D printer using HPMC E15 as a polymer. The polymeric solution was determined by its rheological characteristics. The 3D-printing process was investigated for accuracy by a printability study. The printed ODFs were characterised by a thickness and weight validation, morphological study, crystalline state investigation, disintegration time, mechanical properties, drug content and drug release, and were compared with the ODFs obtained from the casting method.

2. Materials and Methods

2.1. Materials

The mirtazapine (1,2,3,4,10,14b-hexahydro-2-methylpyrazino [2,1-a] pyrido [2,3-c] benzazepine), of USP grade, was purchased from Jiyan Chemicals (Surat, Gujarat, India). The hydroxypropyl methylcellulose E15 (HPMC E15, AnyCoat[®]-C AN15, substitution type 2910, viscosity 15 mPa·s) was purchased from Lotte Fine Chemical Co., Ltd. (Seoul, Korea). The absolute ethanol, citric acid monohydrate, disodium hydrogen phosphate (Na₂HPO₄), sodium chloride (NaCl), potassium phosphate monobasic (KH₂PO₄), and hydrochloric acid were purchased from RCI Labscan (Bangkok, Thailand). The potassium phosphate monobasic (KH₂PO₄) was purchased from Daejung Chemicals (Siheung, Korea). All the other reagents were of analytical grade.

2.2. Rheological Characterization

The rheological behaviour of the formulations was investigated by the Brookfield Plate/Plate Rheometer (Brookfield Rheometer R/S, P25 DIN plate, Brookfield Engineering Laboratories, Middleboro, MA, USA). The instrument was operated in the variation of shear rate from 0–100 s⁻¹ at 25 °C [16]. The distance between the upper plate and lower plate was 1 mm. Each sample measurement was repeated three times. The flow behaviour index (*n*) and consistency coefficient (K) were calculated by the power-law model in the Equation (1).

$$\tau = K\dot{\gamma}^n \quad (1)$$

where τ is the shear stress (Pa), $\dot{\gamma}$ is shear rate (s⁻¹), and K is the consistency coefficient (Pa·s^{*n*})

2.3. Oral Fast-Dissolving Film Loading Mirtazapine Preparation

To prepare the polymeric solution, the hydroxypropyl methylcellulose E15 (HPMC E15), 1.25 g, and citric acid monohydrate, 0.2 g, were dissolved in ethanol:water (9:1), 10 mL, at room temperature, respectively. Then, the polymeric solution was allowed to stand at room temperature for 24 h to eradicate any bubbles.

2.3.1. Casting Method

In the casting method, the MTZ, 0.76 g, was dissolved in 10 mL of the HPMC E15 solution at room temperature. One millilitre of the solution was casted on the glass mould and allowed to stand at room temperature to obtain the dry films. The casted film was cut to obtain a circle of 2 cm in diameter to obtain the film containing 15 mg of MTZ.

2.3.2. 3D-Printing Method

In preparation with a syringe extruder 3D printer, 1.5 g of MTZ was dissolved in 10 mL of the HPMC E15 solution at room temperature. A circle film of 2 cm in diameter was design by Tinkercad software (Autodesk, San Rafael, CA, USA) to obtain 15 mg of the drug content. The printed, oral fast-dissolving film was designed in a dimension of 2 cm diameter × 0.5 cm height. The ODFs were fabricated by a syringe extrusion 3D printer (Biomedical Engineering Institute of Chiang Mai University, Chiang Mai, Thailand). The extrusion nozzle, moving on the X, Y, and Z axes, is controlled by the printer and software. The building plate on the Z-axis is separated to prevent vibration of the sample during the layer-by-layer printing to generate the 3D structure [16]. The polymeric solution in the syringe is pressed through the nozzle by a stepper motor with a direct-lead screw drive. The volume of the printing material was 0.1 mL, and two layers were printed. The polymeric solution containing MTZ as the printing material was loaded into a 10 mL syringe. The material was extruded though a needle (no. 21 G, 0.51 mm in internal diameter) at 0.2 mL/min, and the height between the needle and the glass plate was set at 0.5 mm. The printing speed and nozzle traveling speed were set at 10 and 120 mm/s, respectively. The printing parameters were pre-set with the following conditions: 0.5 mm of layer height,

45° of fill angle, 2 perimeters, and 100% infill. The temperature was controlled at 25 °C. In the measurement of the filament diameter, the infill was set at 0%, and the perimeter was 1. The printed film was dried at room temperature.

2.4. Printability Study

The method to evaluate the accuracy of the printing process is described in Panraksa et al. [16]. The photos of the diameter of the printed filament and surface area of the ODFs were taken by a digital camera (Canon EOS 750D with an 18–55 mm lens, Canon, Inc., Tokyo, Japan) and measured by ImageJ software version 1.52 (National Institutes of Health, Bethesda, MD, USA; available at <https://imagej.nih.gov/ij/index.html> (accessed on 1 July 2022)). The dimension accuracy was reported in terms of the shape fidelity factor (SFF), calculated by Equation (2).

$$\text{Shape fidelity factor (SFF)} = \frac{\text{Printed area (cm}^3\text{)}}{\text{Computer – aided design area (cm}^3\text{)}} \quad (2)$$

2.5. Thickness and Weight Validation

To validate the thickness and weight of the ODFs, the samples were selected randomly. The thickness of the film circle was measured by an outside micrometre (3203-25A, Insize Co, Ltd., Suzhou, China) at three different points. To measure the weight of the ODFs, the sample was weighed by an analytical balance (PA214, Ohaus Corporation, Parsippany, NJ, USA). Each sample was measured three times.

2.6. Morphological Characterization

The surface and cross-section structure of the ODFs were investigated by scanning electron microscopy (SEM) with a JEOL scanning electron microscope (JSM-5410LV, JEOL, Ltd., Peabody, MA, USA) at 10 kV under the low-vacuum mode. The surface and cross-section were observed without coating at magnifications of 200× and 100×, respectively.

2.7. X-Ray Powder Diffractometry (XRD)

The crystalline state of the drug in the ODFs was investigated using an X-ray diffractometer (Miniflex II, Rigaku corporation, Tokyo, Japan). The method was adapted from Naureen et al. [18]. The experiment was performed at a voltage rate of 40 kV. The scanning angle was increased from 5° to 70° at 0.4 s/step of the counting rate. The film samples were fixed with sample holder with a hole (10 mm in diameter). The distance between the sample and the holder was 10 mm. The instrument was operated at a probe speed of 2 mm/s [19].

2.8. In Vitro Disintegration Time

The method to determine the disintegration time was adapted from [20]. The ODF was fixed with a sample holder. A magnetic clip having a weight of 3 g or 0.03 N, referring to minimum applied force of human tongue [20]. The half of a fixed ODF was immersed in 70 mL of stimulated salivary fluid (SSF) pH 6.8 at 37 ± 5 °C. The disintegration time was recorded when the film broke and the magnetic clip dropped down. Each experiment was repeated three times.

2.9. Mechanical Properties Test

The ODFs' mechanical characteristics were evaluated by a texture analyser TX.TA plus (Stable Micro Systems, Surrey, UK) with a load cell of 5 kg (0.001 N of sensitivity) in the compression mode. The sample was compressed by the plane flat-faced surface probe (2 mm in diameter). Each experiment was performed six times. The tensile strength, elongation at break, and Young's modulus were calculated by the equation described in studies of Preis et al. and Chaiwarit et al. [21].

2.10. MTZ Content

The standard curve was obtained by mixing the MTZ solution in 0.1 N HCl in the concentrations of 10, 15, 20, and 25 µg/mL, respectively. The mirtazapine ODFs were completely dissolved in 30 mL of 0.1 N HCl at room temperature. The sample solution was aliquoted into 0.1 mL samples and diluted with 4.9 mL of 0.1 N HCl. The amount of mirtazapine in the sample was measured at 315 nm by a UV–Vis spectrophotometer (UV-2600i, Shimadzu, Kyoto, Japan).

2.11. In Vitro MTZ Release Profile

The in vitro MTZ-release profile of the mirtazapine ODFs was investigated in 1 N HCl. The mirtazapine ODFs were placed in 20 mL of each medium at 37 ± 0.5 °C, with stirring by a magnetic stirrer at 50 rpm. The sample was taken from the media at 0.5, 1, 3, 5, 10, 15, 30, and 60 min, respectively. One hundred thirty-three microliters (133 µL) of the sample solution was diluted to 5 mL, and the amount of MTZ was determined by the UV–Vis spectrophotometer at 315 nm.

2.12. Statistical Analysis

The results were presented as the mean \pm S.D. The SPSS software (version 17; IBM corporation, New York, NY, USA) was used to analyse the significant differences of the analysed results with a 0.05 significance level ($p < 0.05$).

3. Results and Discussion

3.1. Rheological Characteristic

The rheological characteristic of a polymeric solution is a crucial factor in extruding the polymeric solution through the nozzle of a syringe-based 3D printer. The rheological behaviour of the HPMC E15 solution for the 3D printing (3D-MTZ), casting (C-MTZ), and the polymeric solution without the mirtazapine (blank) is shown in Figure 2. The plot between the apparent viscosity and the shear rate demonstrates that all of the formulations showed non-Newtonian rheology with shear-thinning. This means that the apparent viscosity decreases when the shear rate increases during steady shear flow [22]. The parameters from the power-law model fitting are shown in Table 1. The flow-behaviour index (n) of the 3D-MTZ, C-MTZ, and blank were 0.67, 0.72, and 0.74, respectively. The $n < 1$ indicated the non-Newtonian rheology with shear-thinning. This property is suitable for extrusion-based 3D printers because a syringe's polymeric solution can be pressed through the nozzle to print a 3D object [23]. Furthermore, the n slightly decreased with the increase of mirtazapine. This indicated that an additional amount of mirtazapine in the HPMC E15 solution might induce the flow behaviour to be more pseudoplastic (shear thinning). The consistency coefficient values of the 3D-MTZ, C-MTZ, and blank were 59.38, 43.69, and 34.74, respectively. The 3D-MTZ containing the highest amount of mirtazapine possessed the highest viscosity. In other words, increasing the mirtazapine in the HPMC E15 solution possibly increased the solution's apparent viscosity.

3.2. Printability of the Formulations

The filament diameter of all the printed formulations is shown in Figure 3. According to Table 1, the diameter of the printed filament of the 3D-MTZ (0.56 ± 0.01 mm) was approximately the nozzle diameter (0.51 mm), due to the higher viscosity, while the blank, possessing a lower viscosity, exhibited a larger printed filament diameter (0.90 ± 0.02 mm), significantly deviating from the nozzle diameter, than did the 3D-MTZ ($p < 0.05$). This result was also found in our previous study. Panraksa et al. [16] summarized that an appropriate increase in the viscosity value of the polymeric solution could improve printed ODFs to be more accurate and precise. The SFF in all the printed formulations (3D-MTZ and blank) were very close to 1. It meant that a gel filament with a stable shape was deposited in the designed place at the time of extrusion [16]. In other words, it indicated that the printing process was highly accurate.

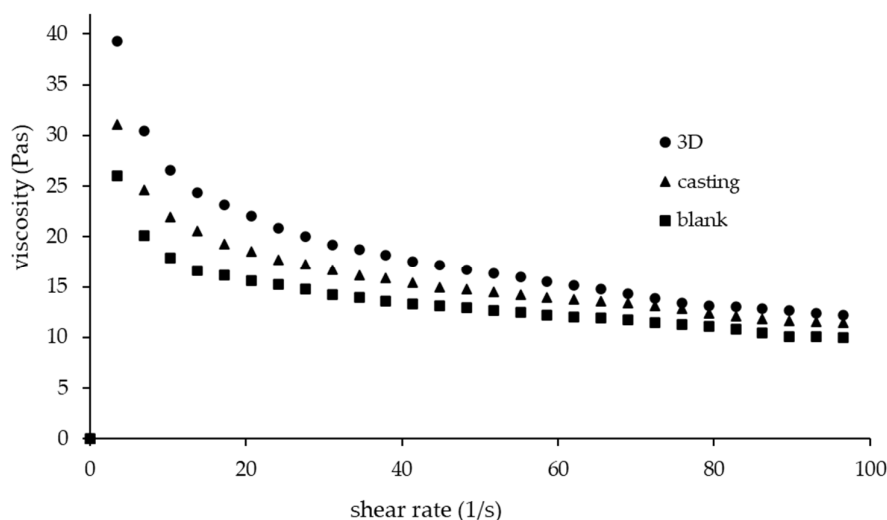


Figure 2. Rheological characteristics of HPMC E15 in different formulations: graph plotted between viscosity and shear rate with fitting power-law model.

Table 1. Parameters from power-law model and shape fidelity factor.

Formulations	Flow Behaviour Index (<i>n</i>)	Consistency Coefficient (Pa.s)	Shape Fidelity Factor	Diameter of Printed Filament (mm)
3D-MTZ	0.67	59.38	1.05 ± 0.04 ^a	0.56 ± 0.01 ^a
C-MTZ	0.72	43.69	NA	NA
Blank	0.74	34.74	1.01 ± 0.08 ^a	0.90 ± 0.02 ^b

Note: NA is not applicable; Different superscript letters in each column indicate significant different (*p* < 0.05).

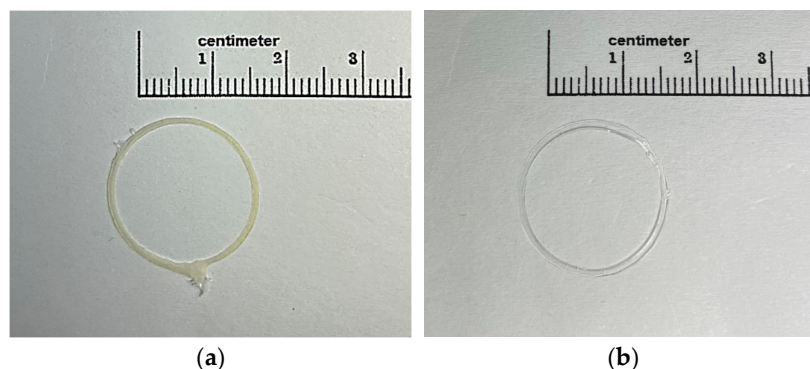


Figure 3. Printed filament diameter of 3D-MTZ (a) and blank (b).

3.3. Morphology of ODFs

The naked eye inspection found that the 3D-MTZ and C-MTZ ODFs were white circles, due to the drug dispersion, while the 3D-blank and C-blank ODFs were transparent and colourless (Figure 4). The printed filament networks from the printing process were clearly observed in the 3D-printed films (3D-MTZ and 3D-blank), but the casted films (C-MTZ and C-blank) were homogenous. The SEM micrographs of the 3D-MTZ, 3D-blank, C-MTZ, and C-blank are shown in Figure 4. Overall, the ODFs appeared homogenous and continuous. In the cross-section observation at 100× magnification, the 3D-MTZ and C-MTZ showed a rough texture, because the crystalline structure of mirtazapine may result in the formation of a rough texture in the film’s matrix [24]. Furthermore, the ODFs produced by the 3D printer were more porous than the casted ODFs because the 3D-printing pattern connected each polymeric filament to a 3D object. An ideal surface morphology indicating a good

quality of ODFs should demonstrate an absence of pores and a surface uniformity [25]. The film's surface observation at 200× magnification exhibited an unbroken surface without any pores, and all the ODFs showed a uniformity of the film surface. In addition, the crystalline MTZ homogeneously disperses on the surfaces of the 3D-MTZ and C-MTZ. On the other hand, the ODFs without the mirtazapine showed a smooth surface.

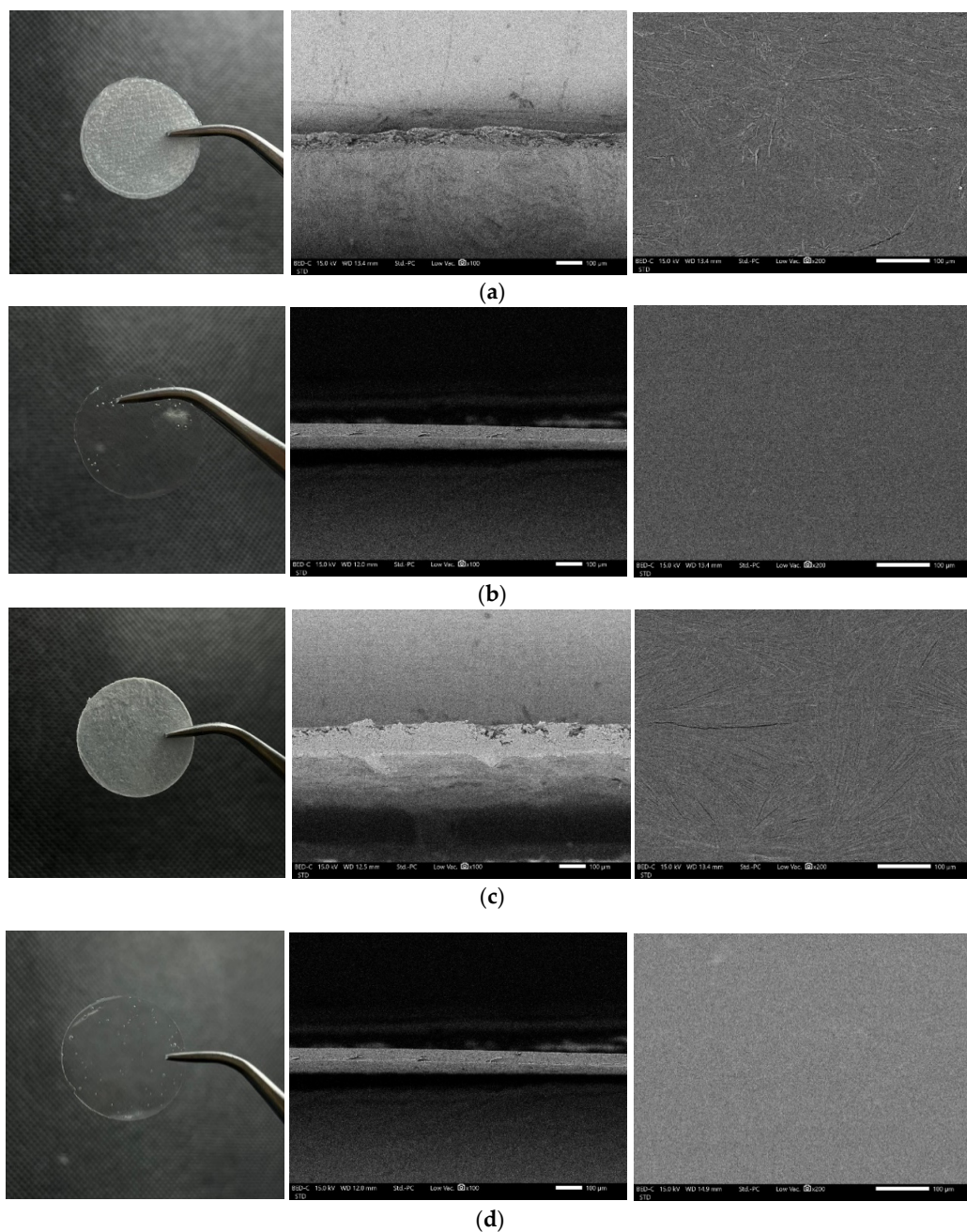


Figure 4. Visual appearances and SEM micrographs of 3D-MTZ (a), 3D-blank (b), C-MTZ (c), and C-blank (d).

3.4. Thickness and Weight Variation of ODFs

The thickness and weight uniformity refer to the accuracy and precision of the preparation process. Generally, the ideal thickness of an oral thin film should be around 0.05–1 mm [26]. The thickness of the 3D-MTZ, C-MTZ, 3D-blank, and C-blank was 0.128 ± 0.009 , 0.145 ± 0.004 , 0.104 ± 0.032 , and 0.074 ± 0.019 mm, respectively (Table 2). The thickness significantly increased when the drug was incorporated into the formula-

tion ($p < 0.05$). However, a significant difference between the thickness of the 3D printing and the casting methods was not observed ($p > 0.05$). To confirm that the amount of drug-loading in each film is an insignificant deviation, the weight variation should be evaluated [24]. In our study, the weight of the 3D-MTZ, C-MTZ, 3D-blank, and C-blank ODFs was 0.0344 ± 0.0006 , 0.0515 ± 0.0005 , 0.0308 ± 0.0042 , and 0.0252 ± 0.0034 g, respectively (Table 2). The weight of the ODFs increased with the addition of the MTZ. In addition, the printed ODFs showed less standard deviation than the casted ODFs. This indicated that the 3D-printing process was more precise than the casting method.

Table 2. Thickness, weight, and mechanical properties of ODFs.

Formulations	Thickness (mm)	Weight (g)	Puncture Strength (N/mm ²)	Elongation at Break (%)	Young's Modulus (N/mm ²)
3D-MTZ	0.128 ± 0.008 ^a	0.0344 ± 0.0006 ^a	1.11 ± 0.05 ^a	5.39 ± 0.67 ^a	22.06 ± 0.95 ^a
C-MTZ	0.145 ± 0.004 ^b	0.0515 ± 0.0045 ^b	1.53 ± 0.13 ^b	1.55 ± 0.36 ^b	27.89 ± 3.66 ^b
3D-blank	0.104 ± 0.012 ^c	0.0308 ± 0.0012 ^c	3.30 ± 0.49 ^c	12.61 ± 1.55 ^c	62.03 ± 2.84 ^c
C-blank	0.074 ± 0.019 ^c	0.0252 ± 0.0034 ^d	4.92 ± 0.51 ^d	12.79 ± 0.40 ^c	98.13 ± 2.74 ^d

Note: Different superscript letters in each column indicate significant different ($p < 0.05$).

3.5. Mechanical Properties of ODFs

The mechanical properties refer to the elasticity of the ODFs and confirm that the ODFs have appropriate physical characteristics to handle and remove from the packaging. The mechanical properties of all the ODFs are shown in Table 2. The puncture strength of the 3D-MTZ (1.11 ± 0.01 N/mm²) and C-MTZ (1.33 ± 0.13 N/mm²) were insignificantly different to each other ($p > 0.05$). However, the puncture strength and elongation at break significantly decreased and increased, respectively, with the MTZ addition ($p < 0.05$). For example, the puncture strength and elongation at break of the 3D-MTZ was 1.11 ± 0.01 N/mm² and $5.39 \pm 0.67\%$, respectively, while the 3D-blank exhibited 3.30 ± 0.49 N/mm² and $12.61 \pm 1.55\%$ of puncture strength and elongation at break, respectively. These results were caused by the drug incorporation. The MTZ, added into the film's matrix, interferes with the polymer–polymer interaction, leading to the rearrangement of the polymer chains to alter the mechanical properties (to be less hard and decrease the ability to stretch, respectively) [27]. The possible interaction between the MTZ and HPMC might be hydrogen bonding, because the N⁺ atom of MTZ could form with the H atom of -OH in the HPMC molecule to form N⁺-H...O bonds [28]. Furthermore, the puncture strength and elongation at break of the 3D-blank (1.11 ± 0.01 N/mm² and $5.39 \pm 0.67\%$) were significantly lower and higher than the C-blank (1.33 ± 0.13 N/mm² and $1.55 \pm 0.36\%$), respectively, because of the preparation processes. The structure of the casted films was continuous and dense, while the printed films had pores that could decrease the puncture strength and increase the elongation at break [29]. Young's modulus of the printed ODFs was significantly lower than the casted ODFs. For example, Young's modulus of the 3D-blank was 62.03 ± 2.84 N/mm², whereas the C-blank exhibited 98.13 ± 2.74 N/mm² of Young's modulus. It also could be explained by the 3D-printing fabricating porous films [29]. Young's modulus also significantly decreased when the drug was incorporated, due to the rearrangement of the polymer chains [27]. Thus, the 3D-MTZ showed the lowest Young's modulus (22.06 ± 0.95 N/mm²), which meant it was less rigid than the other formulations.

3.6. X-Rays Powder Diffractometry

The diffractograms of the MTZ powder, HPMC E15, 3D-MTZ, and C-MTZ are shown in Figure 5. The diffractogram of the mirtazapine powder shows some peaks at 9.25, 14.39, 18.57, 19.24, 20.38, 21.81, 23.68, 25.86, 26.77, etc. (Figure 5a). These peaks indicate the crystalline form of the drug and were also found in Naureen et al. [18]. Controversially, the diffractogram of the HPMC E15 shows an amorphous pattern, without any peaks of crystalline structure (Figure 5b). The diffractograms of the 3D-MTZ and C-MTZ show a

mixed pattern between the MTZ powder and the HPMC E15. Furthermore, some specific peaks, such as the peaks at 19.25 and 26.77 2θ , disappeared. This result indicates that the crystalline structure of the drug partially converted to an amorphous state. When a solvent evaporates, the drug dispersed in a polymeric carrier can change to an amorphous form [30,31]. In other words, the 3D-printing and casting, involving solvent evaporation, could reduce the drug's crystallization [32]. In addition, the remaining drug crystals appeared on the ODFs surface, as observed in the SEM micrographs.

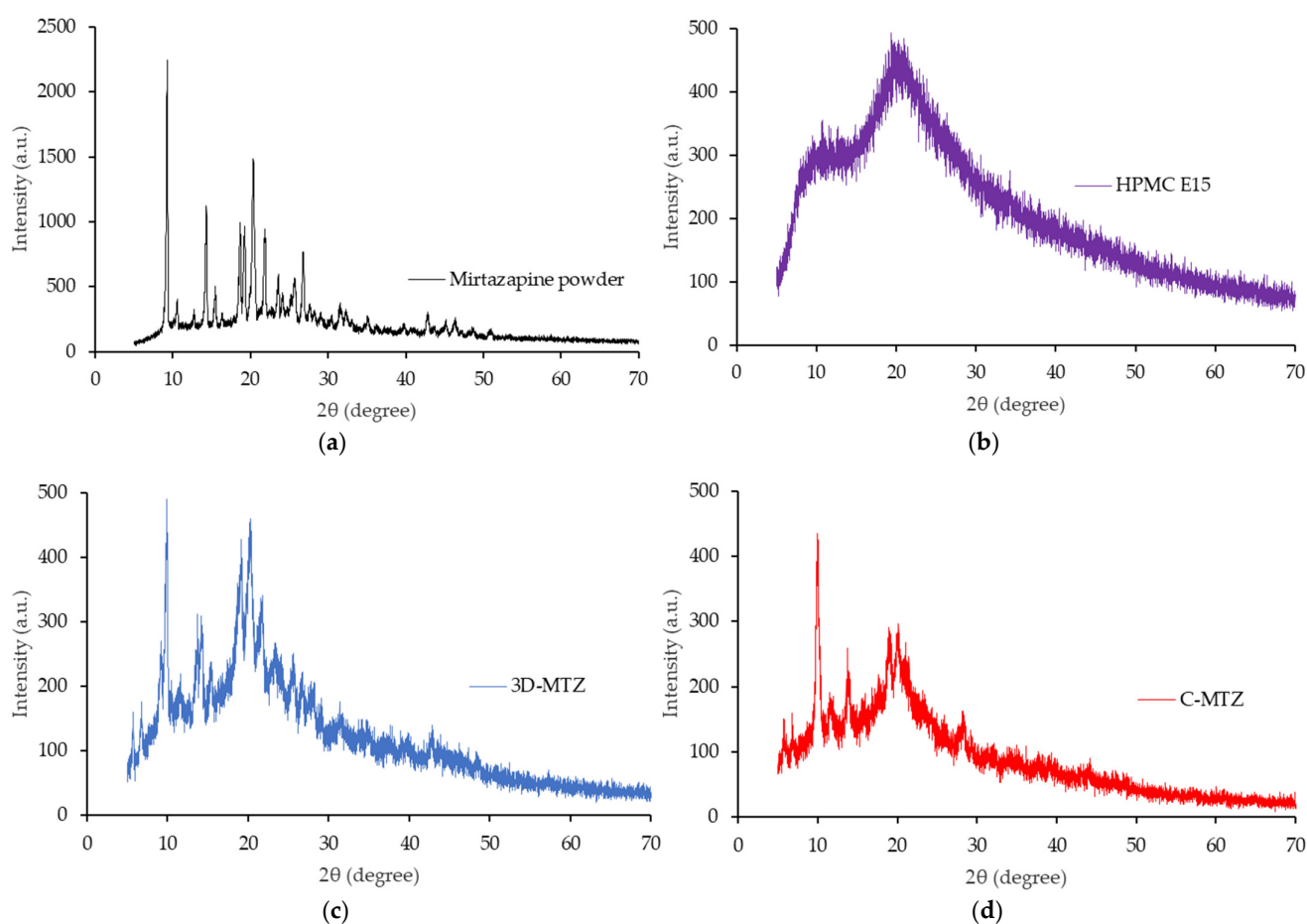


Figure 5. Diffractograms of mirtazapine powder (a), HPMC E15 (b), 3D-MTZ (c) and C-MTZ (d).

3.7. Disintegration Time of ODFs

The in vitro disintegration times of all the ODFs are shown in Table 3. Currently, the disintegration time of ODFs is not specified by any guidance in an official pharmacopoeia. However, the United States Pharmacopeia (USP) and The Center for Drug Evaluation and Research (CDER) guidance specifies that oral disintegrating tablets should disintegrate in 30 s, which may be applied to ODFs [33]. Our results showed that the disintegration time was longer with an increase of the film's thickness. To clarify, the thicker films have less surface area to contact with the medium than the thinner films. Thus, it is possible that the thinner ODFs provide a faster disintegration time. In addition, the MTZ-loaded ODFs showed a slower disintegration time than the blank film because of the insoluble nature of the drug substance [29]. Interestingly, the disintegration time of the 3D-MTZ was 24.38 ± 1.53 s, but the C-MTZ exhibited a significantly longer disintegration time (46.75 ± 2.52 s) of more than 30 s ($p < 0.05$). In addition, the porous structure and gaps between each printed filament produced by 3D printing may contribute to a faster disintegration [34].

Table 3. Disintegration time and MTZ content of ODFs.

Formulations	Disintegration Time (s)	MTZ Content (%)
3D-MTZ	24.38 ± 1.53 ^a	106.25 ± 3.85 ^a
C-MTZ	46.75 ± 2.52 ^b	100.74 ± 1.80 ^a
3D-blank	17.85 ± 1.87 ^c	NA
C-blank	15.26 ± 1.17 ^c	NA

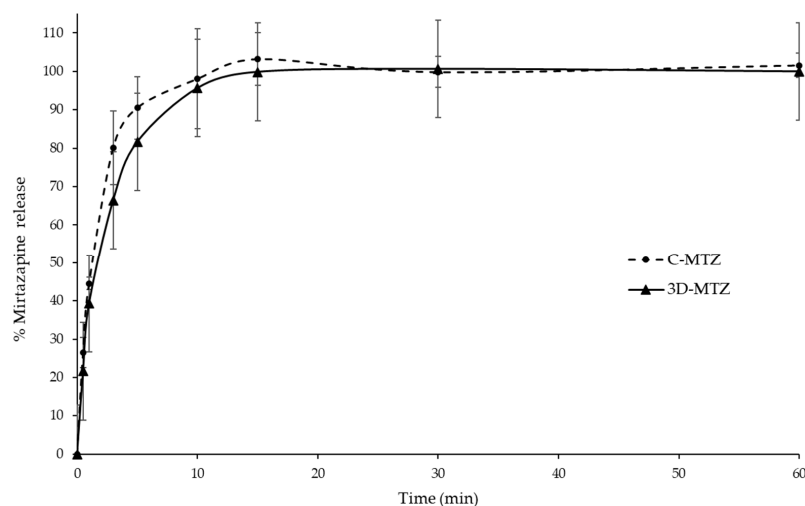
Note: NA is not applicable; different superscript letters in each column indicate significant different ($p < 0.05$).

3.8. MTZ Content

The uniformity of the incorporated drug in ODFs refers to the robustness and precision of the film preparation process. In our study, the theoretical MTZ content in circle ODFs (2 cm diameter) was 15 mg. The mirtazapine content of the 3D-MTZ and C-MTZ was 106.25 ± 3.85 and $100.74 \pm 1.80\%$, respectively (Table 3). According to USP 43 NF38, the acceptance criteria for mirtazapine in a pharmaceutical dosage form were 90–110% [35]. Thus, the MTZ content of the 3D-MTZ and C-MTZ complied with the USP specification. These results confirmed the uniformity of the MTZ in ODFs and indicated both the syringe extrusion 3D printer and casting method were precise in producing the ODFs.

3.9. MTZ Release Profile

According to USP 43 NF38, the drug release profile of MTZ must be performed in 1 N HCl because the MTZ is normally absorbed in the stomach. The MTZ release profile is shown in Figure 6. Overall, the percentage of drug release of the 3D-MTZ was not significantly different from the C-MTZ ($p > 0.05$), although the 3D-MTZ had a faster disintegration time than the C-MTZ. Both the 3D-MTZ and C-MTZ released the drug rapidly and by more than 80% in 5 min, then gradually released to around 95% at 10 min. Another study found that MTZ disintegrating tablets showed an 85% drug release in 1 N HCl at 15 min [36]. The MTZ–HPMC interaction may be involved with the drug release. The possible interaction between the MTZ and HPMC is the hydrogen bonding ($N^+-H \cdots O$ bonds). In a polar environment, hydrogen bonds are weak and can be broken easily, due to the disturbance of the water molecule. Furthermore, the O atom of the water molecule could competitively form a hydrogen bond with the N atom of the mirtazapine molecule [37]. Thus, the ODFs in our study showed a faster drug release and potential to be used as an orally fast-disintegrating formulation. Another reason to explain the rapid drug release is the nature of crystalline structures. The mirtazapine crystals in the 3D-MTZ and C-MTZ partially convert to an amorphous state that might increase the water solubility of the mirtazapine. This study indicated that the 3D printing and casting produced ODFs with a rapid drug release.

**Figure 6.** The release profile of MTZ from ODFs in 1 N HCl.

4. Conclusions

Our study successfully fabricated ODFs containing mirtazapine by a syringe extrusion 3D printer. The loaded mirtazapine affected the rheology and provided an excellent printability. The 3D-printing technique is a highly accurate and precise method to produce ODFs. The ODFs obtained from the 3D printing showed a porous matrix, affecting the film's properties. The printed ODFs showed better mechanical properties and faster disintegration times in SSF pH 6.8 than the casted films and disintegrated in 24.38 s. The XRD study found both the 3D printing and casting methods could partially convert the crystalline structure of mirtazapine. In addition, the 3D printed ODFs delivered a high drug content with accuracy and could immediately release more than 80% of the drug in 5 min. Overall, this study indicated that syringe extrusion 3D printing using HPMC E15 as a polymer can produce ODFs. In the future, further experiments, such as ODFs' stability, personalized dosage adjustments and different polymer comparisons, will be investigated to fulfil this research.

Author Contributions: Conceptualisation, T.C. and P.J.; investigation, T.C., N.A., P.P. (Pimonnart Promyos), P.P. (Pattaraporn Panraksa) and P.J.; methodology, T.C., N.A., P.P. (Pimonnart Promyos), P.P. (Pattaraporn Panraksa), S.U. and P.J.; validation, T.C. and P.J.; writing—original draft, T.C. and P.J.; writing—review & editing, T.C. and P.J. All authors have read and agreed to the published version of the manuscript.

Funding: This research was partially supported by Chiang Mai University.

Institutional Review Board Statement: Not applicable.

Informed Consent Statement: Not applicable.

Data Availability Statement: Not applicable.

Acknowledgments: The authors would like to thank the Complementary Medicine Health Products Research and Development Center, Pharmacy Department, Suanprung Psychiatric Hospital, Chiang Mai, Thailand, for providing the mirtazapine drug sample.

Conflicts of Interest: The authors declare no conflict of interest.

References

1. World health organization (WHO). Depression. Available online: <https://www.who.int/news-room/fact-sheets/detail/depression> (accessed on 3 October 2022).
2. Matreja, P.S.; Badyal, D.K.; Deswal, R.S.; Sharma, A. Efficacy and safety of add on low-dose mirtazapine in depression. *Indian J. Pharmacol.* **2012**, *44*, 173–177. [[PubMed](#)]
3. Papakostas, G.I.; Homberger, C.H.; Fava, M. A meta-analysis of clinical trials comparing mirtazapine with selective serotonin reuptake inhibitors for the treatment of major depressive disorder. *J. Psychopharmacol.* **2008**, *22*, 843–848. [[CrossRef](#)] [[PubMed](#)]
4. Ezealisiji, K.E.; Mbah, C.J.; Osadebe, P.O. Aqueous Solubility Enhancement of Mirtazapine: Effect of Cosolvent and Surfactant. *Pharmacol. Pharm.* **2015**, *6*, 471–476. [[CrossRef](#)]
5. Meineke, I.; Steinmetz, H.; Kirchheiner, J.; Brockmöller, J. Therapeutic drug monitoring of mirtazapine, desmethylmirtazapine, 8-hydroxymirtazapine, and mirtazapine-N-oxide by enantioselective HPLC with fluorescence detection. *Ther. Drug Monit.* **2006**, *28*, 760–765. [[CrossRef](#)] [[PubMed](#)]
6. Sjöholm, E.; Sandler, N. Additive manufacturing of personalized orodispersible warfarin films. *Int. J. Pharm.* **2019**, *564*, 117–123. [[CrossRef](#)]
7. Musazzi, U.M.; Selmin, F.; Ortenzi, M.A.; Mohammed, G.K.; Franzé, S.; Minghetti, P.; Cilirzo, F. Personalized orodispersible films by hot melt ram extrusion 3D printing. *Int. J. Pharm.* **2018**, *551*, 52–59. [[CrossRef](#)]
8. Speer, I.; Preis, M.; Breikreutz, J. Prolonged drug release properties for orodispersible films by combining hot-melt extrusion and solvent casting methods. *Eur. J. Pharm. Biopharm.* **2018**, *129*, 66–73. [[CrossRef](#)]
9. Krause, J.; Bogdahn, M.; Schneider, F.; Koziolok, M.; Weitschies, W. Design and characterization of a novel 3D printed pressure-controlled drug delivery system. *Eur. J. Pharm. Sci.* **2019**, *140*, 105060. [[CrossRef](#)]
10. Ngo, T.D.; Kashani, A.; Imbalzano, G.; Nguyen, K.T.Q.; Hui, D. Additive manufacturing (3D printing): A review of materials, methods, applications and challenges. *Compos. B. Eng.* **2018**, *143*, 172–196. [[CrossRef](#)]
11. Redekop, W.K.; Mladi, D. The Faces of Personalized Medicine: A Framework for Understanding Its Meaning and Scope. *Value Health* **2013**, *16*, S4–S9. [[CrossRef](#)]

12. Cerda, J.R.; Arifi, T.; Ayyoubi, S.; Knief, P.; Ballesteros, M.P.; Keeble, W.; Barbu, E.; Healy, A.M.; Lalatsa, A.; Serrano, D.R. Personalised 3D Printed Medicines: Optimising Material Properties for Successful Passive Diffusion Loading of Filaments for Fused Deposition Modelling of Solid Dosage Forms. *Pharmaceutics* **2020**, *12*, 345. [[CrossRef](#)] [[PubMed](#)]
13. Azad, M.A.; Olawuni, D.; Kimbell, G.; Badruddoza, A.Z.M.; Hossain, M.S.; Sultana, T. Polymers for Extrusion-Based 3D Printing of Pharmaceuticals: A Holistic Materials–Process Perspective. *Pharmaceutics* **2020**, *12*, 124. [[CrossRef](#)] [[PubMed](#)]
14. Dixit, R.P.; Puthli, S.P. Oral strip technology: Overview and future potential. *J. Control. Release* **2009**, *139*, 94–107. [[CrossRef](#)] [[PubMed](#)]
15. Dahiya, M.; Saha, S.; Shahiwala, F.A. A Review on Mouth Dissolving Films. *Curr. Drug Deliv.* **2009**, *6*, 469–476. [[CrossRef](#)] [[PubMed](#)]
16. Panraksa, P.; Udomsom, S.; Rachtanapun, P.; Chittasupho, C.; Ruksiriwanich, W.; Jantrawut, P. Hydroxypropyl Methylcellulose E15: A Hydrophilic Polymer for Fabrication of Orodispersible Film Using Syringe Extrusion 3D Printer. *Polymers* **2020**, *12*, 2666. [[CrossRef](#)]
17. Yan, T.T.; Lv, Z.F.; Tian, P.; Lin, M.M.; Lin, W.; Huang, S.Y.; Chen, Y.Z. Semi-solid extrusion 3D printing ODFs: An individual drug delivery system for small scale pharmacy. *Drug Dev. Ind. Pharm.* **2020**, *46*, 531–538. [[CrossRef](#)]
18. Naureen, F.; Shah, Y.; Shah, S.I.; Abbas, M.; Rehman, I.U.; Muhammad, S.; Hamdullah, H.; Goh, K.W.; Khuda, F.; Khan, A.; et al. Formulation Development of Mirtazapine Liquisolid Compacts: Optimization Using Central Composite Design. *Molecules* **2022**, *27*, 4005. [[CrossRef](#)]
19. Junmahasathien, T.; Panraksa, P.; Protiarn, P.; Hormdee, D.; Noisombut, R.; Kantrong, N.; Jantrawut, P. Preparation and Evaluation of Metronidazole-Loaded Pectin Films for Potentially Targeting a Microbial Infection Associated with Periodontal Disease. *Polymers* **2018**, *10*, 1021. [[CrossRef](#)]
20. Preis, M.; Knop, K.; Breitreutz, J. Mechanical strength test for orodispersible and buccal films. *Int. J. Pharm.* **2014**, *461*, 22–29. [[CrossRef](#)]
21. Chaiwarit, T.; Rachtanapun, P.; Kantrong, N.; Jantrawut, P. Preparation of Clindamycin Hydrochloride Loaded De-Esterified Low-Methoxyl Mango Peel Pectin Film Used as a Topical Drug Delivery System. *Polymers* **2020**, *12*, 1006. [[CrossRef](#)]
22. Cooke, M.; Rosenzweig, D. The rheology of direct and suspended extrusion bioprinting. *APL Bioeng.* **2021**, *5*, 011502. [[CrossRef](#)] [[PubMed](#)]
23. Polamapilly, P.; Cheng, Y.; Shi, X.; Manikandan, K.; Zhang, X.; Kremer, G.E.; Qin, H. 3D printing and characterization of hydroxypropyl methylcellulose and methylcellulose for biodegradable support structures. *Polymer* **2019**, *173*, 119–126. [[CrossRef](#)]
24. Karki, S.; Kim, H.; Na, S.-J.; Shin, D.; Jo, K.; Lee, J. Thin films as an emerging platform for drug delivery. *Asian J. Pharm. Sci.* **2016**, *11*, 559–574. [[CrossRef](#)]
25. Irfan, M.; Rabel, S.; Bukhtar, Q.; Qadir, M.I.; Jabeen, F.; Khan, A. Orally disintegrating films: A modern expansion in drug delivery system. *Saudi Pharm. J.* **2016**, *24*, 537–546. [[CrossRef](#)]
26. Nair, A.B.; Kumria, R.; Harsha, S.; Attimarad, M.; Al-Dhubiab, B.E.; Alhaider, I.A. In vitro techniques to evaluate buccal films. *J. Control. Release* **2013**, *166*, 10–21. [[CrossRef](#)] [[PubMed](#)]
27. Centkowska, K.; Ławrecka, E.; Sznitowska, M. Technology of Orodispersible Polymer Films with Micronized Loratadine-Influence of Different Drug Loadings on Film Properties. *Pharmaceutics* **2020**, *12*, 250. [[CrossRef](#)] [[PubMed](#)]
28. Sarkar, A.; Rohani, S. Molecular salts and co-crystals of mirtazapine with promising physicochemical properties. *J. Pharm. Biomed. Anal.* **2015**, *110*, 93–99. [[CrossRef](#)]
29. Jamróz, W.; Kurek, M.; Łyszczarz, E.; Szafraniec, J.; Knapik-Kowalczyk, J.; Syrek, K.; Paluch, M.; Jachowicz, R. 3D printed orodispersible films with Aripiprazole. *Int. J. Pharm.* **2017**, *533*, 413–420. [[CrossRef](#)]
30. Yamashita, K.; Nakate, T.; Okimoto, K.; Ohike, A.; Tokunaga, Y.; Ibuki, R.; Higaki, K.; Kimura, T. Establishment of new preparation method for solid dispersion formulation of tacrolimus. *Int. J. Pharm.* **2003**, *267*, 79–91. [[CrossRef](#)]
31. Oh, D.H.; Park, Y.-J.; Kang, J.H.; Yong, C.S.; Choi, H.-G. Physicochemical characterization and in vivo evaluation of flurbiprofen-loaded solid dispersion without crystalline change. *Drug Deliv.* **2011**, *18*, 46–53. [[CrossRef](#)]
32. Janßen, E.M.; Schliephacke, R.; Breitenbach, A.; Breitreutz, J. Drug-printing by flexographic printing technology—A new manufacturing process for orodispersible films. *Int. J. Pharm.* **2013**, *441*, 818–825. [[CrossRef](#)] [[PubMed](#)]
33. Banarjee, T.; Ansari, V.A.; Singh, S.; Mahmood, T.; Akhtar, J. A review on fast dissolving films for buccal delivery of low dose drugs. *Int. J. Life Sci. Rev.* **2015**, *1*, 117–123.
34. Ehtezazi, T.; Algellay, M.; Islam, Y.; Roberts, M.; Dempster, N.M.; Sarker, S.D. The Application of 3D Printing in the Formulation of Multilayered Fast Dissolving Oral Films. *J. Pharm. Sci.* **2018**, *107*, 1076–1085. [[CrossRef](#)] [[PubMed](#)]
35. USP. *The United States Pharmacopeia*, 43rd ed.; United States Pharmacopeial Convention: Rockville, MD, USA, 2020; p. 2980.
36. Yıldız, S.; Aytakin, E.; Yavuz, B.; Bozdağ Pehlivan, S.; Ünlü, N. Formulation studies for mirtazapine orally disintegrating tablets. *Drug Dev. Ind. Pharm.* **2016**, *42*, 1008–1017. [[CrossRef](#)] [[PubMed](#)]
37. Li, Y.; Yang, L. Driving forces for drug loading in drug carriers. *J. Microencapsul.* **2015**, *32*, 255–272. [[CrossRef](#)] [[PubMed](#)]